Pergamon

Journal of South American Earth Sciences, Vol. 7, No. 2, pp. 149-165, 1994

0895-9811/94 $7.00 + 0.00

0895-9811(94)E0014-R

K-Ar and $^{40}Ar/^{39}Ar$ evidence for a Transamazonian age (2030-1970 Ma) for the granites and emerald-bearing K-metasomatites from Campo Formoso and Carnaíba (Bahia, Brazil)

G. GIULIANI[1,2], J.-L. ZIMMERMANN[2] and R. MONTIGNY[3]

[1]ORSTOM, Département TOA, UR 1H, 213 rue La Fayette -75480 Paris (France).
[2]C.R.P.G.-C.N.R.S., BP.20 -54501 Vandoeuvre (France). [3]E.O.P.G.S., 5 rue Descartes -67084 Strasbourg (France).

(Received April 1993; Revision Accepted December, 1993)

Abstract—The Campo Formoso and Carnaíba granites belong to a suite of middle Proterozoic magmatic rocks located in the northern part of the São Francisco craton. They intrude the Archaean basement and Lower Proterozoic Jacobina volcanosedimentary series. Emerald-bearing K-metasomatites in the mining districts of Campo Formoso and Carnaíba are developed within serpentinites at the contact with granite-related pegmatitic veins.

K-Ar and $^{40}Ar/^{39}Ar$ measurements were performed on biotites and deuteric muscovites from these two granites, and phlogopites from the K-metasomatites. For the Campo Formoso granite, the biotites yield ages between 1875 ± 45 Ma and 1908 ± 47 Ma (2σ) and the muscovites yield ages of 1897 ± 34 Ma and 2040 ± 24 Ma (2σ). For the Carnaíba granite, the biotites and muscovites fit isochrons with ages of 1888 ± 32 and 1979 ± 28 Ma (2σ), respectively. In contrast, phlogopites from emerald-bearing metasomatites display K-Ar ages that spread between 1900 and 2000 Ma with an isochron of 1973 ± 20 Ma (2σ) for Carnaíba. Generally, the youngest biotite and phlogopite ages occur for specimens where these minerals are chloritized. $^{40}Ar/^{39}Ar$ step heating release spectra are complex but give integrated ages in good agreement with the K-Ar ages. The least disturbed spectrum permits assignment of an age of 2032 ± 10 Ma (2σ) for the first granitic pulse of the emplacement of the Campo Formoso composite pluton.

Since in Carnaíba, deuteric muscovites and chlorite-free phlogopites give similar K-Ar ages, 1979 ± 28 and 1973 ± 20 Ma (2σ) respectively, we conclude that emerald mineralization is contemporaneous with the pervasive muscovitization of the granite. The 1979 ± 28 Ma (2σ) age obtained by K-Ar on muscovite represents the best estimate of the Carnaíba granite cooling age. A model invoking the pervasive alteration of the upper part of the granitic cupola along the pegmatite veins and serpentinites by the muscovitizing fluids is proposed for the formation of emerald-bearing K-metasomatites.

The disturbances of $^{40}Ar/^{39}Ar$ release spectra testify to the existence of a hydrothermal heating that overprinted the K-Ar clock of biotite and to a less extent phlogopite. This event is clearly subsequent to the Transamazonian granitization and emerald mineralization and consequently younger than 1973 ± 20 Ma. Due to the lack of structural evidences for a Braziliano event (700-500 Ma) in this region, we tentatively propose a Transamazonian age (1900 Ma) for the thermal overprint.

Resumo—Os granitóides de Campo Formoso e Carnaíba pertencem à uma série de rochas magmáticas do Proterozóico Médio localizadas na parte norte do cráton São Francisco. Estes granitos cortam o embasamento Arqueano e as formações vulcanossedimentares da Serra da Jacobina (Bahia). Os metassomatitos potássicos situados na zona mineira de Campo Formoso e Carnaíba são hospedeiros das mineralizações à esmeralda e se formaram ao longo dos contatos entre pegmatitos relacionados aos granitóides e serpentinitos.

Datações radiométricas K-Ar e $^{40}Ar/^{39}Ar$ foram realizadas sobre biotitas e muscovitas deutéricas dos granitos, e também sobre flogopitas dos metassomatitos potássicos. Para o granito de Campo Formoso, as biotitas definem uma idade situada entre 1875 ± 45 Ma e 1908 ± 47 Ma (2σ), enquanto as muscovitas fornecem idades entre 1897 ± 34 Ma e 2040 ± 24 Ma (2σ). No caso do granito de Carnaíba, as biotitas e as muscovitas definem isócronas de 1888 ± 32 e 1979 ± 28 Ma (2σ), respectivamente. Por outro lado, as idades K-Ar das flogopitas se espalham entre 1900 e 2000 Ma e definem uma isócrona de 1973 ± 20 Ma (2σ) para os metassomatitos de Carnaíba. Geralmente, as idades mas jovem de biotita e flopopita foram obtidas sobre minerais cloritizados. Apesar de complexos, os espectros $^{40}Ar/^{39}Ar$ definem idades integradas que concordam com as idades K-Ar. O espectro meno disturbado permite atribuir uma idade de 2032 ± 10 Ma (2σ) para o primeiro pulso granítico do pluton composto de Campo Formoso.

Considerando que em Carnaíba, as muscovitas deutéricas e as flogopitas não cloritizadas fornecem idades K-Ar similares, 1979 ± 28 Ma e 1973 ± 20 Ma (2σ) respectivamente, pode-se concluir que a mineralização à esmeralda é contemporânea da muscovitização pervasiva que afetou o granito. A idade K-Ar obtida a partir das muscovitas, 1979 ± 28 Ma (2σ), representa a melhor estimativa para a idade de resfriamento do granito de Carnaíba. Um modelo metalogenético baseado na alteração pervasiva da parte superior da cúpula granítica ao longo do contato entre veios pegmatíticos e serpentinitos, por parte dos fluidos muscovitizantes, é proposto para a formação dos metassomatitos potássicos encaixantes das esmeraldas.

A natureza discordante dos espectros $^{40}Ar/^{39}Ar$ reforça a evidência de um aquecimento hidrotermal que causou a abertura do sistema K-Ar das biotitas e das flogopitas. Esse evento termal, que é claramente superimposto aos granitos e aos metassomatitos à esmeralda, é necessariamente considerado como tendo uma idade inferior à 1973 ± 20 Ma. Na ausência de evidências da fase de deformação Brasiliana (700-500 Ma) para esta região, uma idade Transamazônica (1900 Ma) é proposta para esse evento termal.

Address all correspondence and reprint requests to Gaston Giuliani, present address-C.R.P.G.-C.N.R.S., BP.20 -54501 Vandoeuvre (France)

INTRODUCTION

The purpose of this study is to (1) assess for the first time a direct K-Ar age of emerald formation, and (2) establish the time gap between granite-pegmatite emplacement and the metasomatic processes responsible for the emerald mineralization in the mining districts of Campo Formoso and Carnaíba, which are located in the northern part of the São Francisco craton (Fig. 1). To address these questions, we carried out conventional K-Ar replicate analyses and incremental degassing complemented by a few $^{40}Ar/^{39}Ar$ stepwise heating experiments on muscovites and biotites from granites, and on phlogopites from the spatially associated emerald-bearing K-metasomatites. It was expected that K-Ar replicate analyses of high K content-minerals would give sufficient age resolution to distinguish two closely-occurring geologic events. Moreover, the emerald deposits of Campo Formoso and Carnaíba appeared to be well constrained geologically by field investigations (Rudowski *et al.*, 1987), petrographical and geochemical studies (Rudowski, 1989; Giuliani *et al.*, 1990), and Rb-Sr age determinations on granite whole-rock (Torquato et al., 1978; Lafon, 1988; Sabaté et al., 1990) and K-metasomatites (Rudowski, 1989; Vidal et al.,1992).

Previous Rb-Sr radiometric data support the view that the Transamazonian magmatism occurred between 2000-1880 Ma. Torquato *et al.* (1978) determined an age of 1978±24 Ma for the first phase of granitization in Campo Formoso whereas Lafon (1988) obtained a 1881±23 Ma age for the second phase; likewise, Sabaté *et al.* (1990) determined an age of 1969±29 Ma for these two granitic pulses and, an age of 1883±87 Ma for the Carnaíba granite. The emergence of two groups of ages is suggestive of the existence of a probable hydrothermal overprint, which would have occurred subsequent to the granite emplacement. Thus, the question arises whether the emerald mineralization is a by-product of the granite emplacement or is induced by a late hydrothermal overprint.

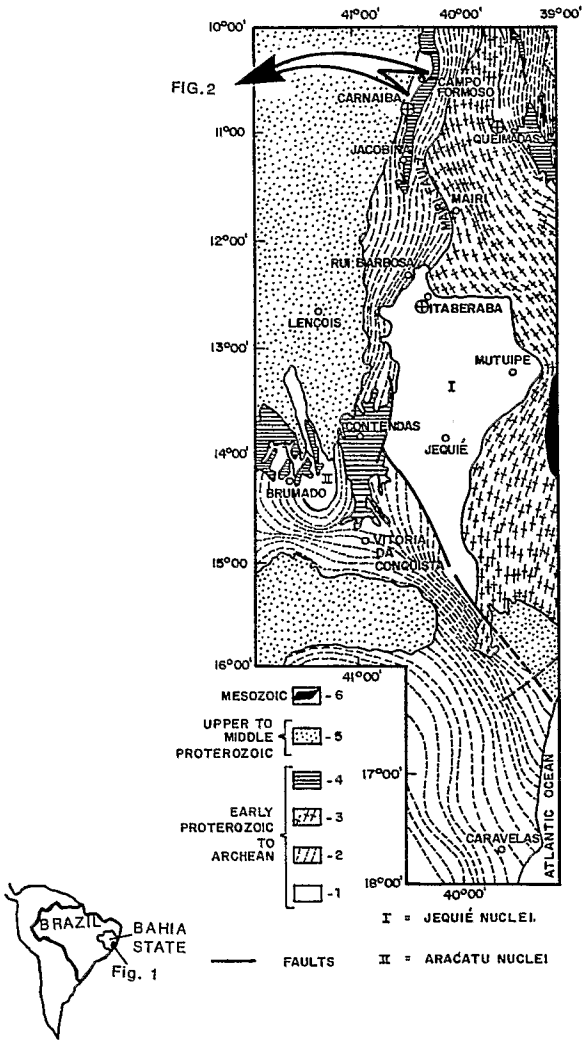

Fig. 1. Simplified geological map of Archaean and Proterozoic terranes of the Bahia State (modified from Mascarenhas, 1979; Cordani and Brito Neves, 1982) showing the location of the Campo Formoso and Carnaíba region. 1=cratonic nuclei (mainly granulitic); 2=granitic-gneissic-migmatitic terranes; 3=Salvador-Juazeiro Mobile Belt (amphibolite to granulite facies); 4=volcanosedimentary sequences; 5=platform sediments of the Brazilian Cycle; 6=Mesozoic sedimentary cover.

GEOLOGICAL SETTING

The granites of Campo Formoso and Carnaíba are located in the northern part of the Precambrian basement of the São Francisco craton (Fig. 1). They intrude both Archaean migmatitic basement and the Lower Proterozoic Jacobina volcanosedimentary series composed mainly of intercalated iron formations, acid, basic and ultrabasic volcanic horizons, cherts and quartzites. Structurally, the Jacobina series appears to be thrust over the Archaean migmatitic basement along a serpentinite basal fault.

The Campo Formoso pluton

The pluton has a concentric structure (Fig. 2A) resulting from a multistage intrusive process. It is composed of a peripheral coarse- to medium-grained two-mica granite (γ1) and a central fine-grained (γ2a) to porphyritic two-mica granite (γ2b). Field relationships between γ1 and γ2 have been clearly established (Rudowski *et al.*, 1987), indicating that γ2 intruded γ1. Several generations of pegmatite veins crosscut both γ1 and γ2. Locally these veins contain beryl, molybdenite and sulphides. Deuteric-hydrothermal alterations are represented by intense muscovitization in both γ1 and γ2, greisenization and tourmalinization in γ1 and K-feldspathization in γ2.

The Carnaíba massif

This circular, 4 km wide granitic stock is emplaced within the core of an antiform structure of the Serra da Jacobina (Fig. 2B). Its intrusive character is demonstrated by the presence of serpentinite roof pendants and quartzite enclaves in the granite. The stock consists of a two-mica granite (γCA), which is cross-cut by a dense swarm of garnet-cordierite-muscovite-bearing pegmatite veins. Muscovitization and chloritization are pervasive.

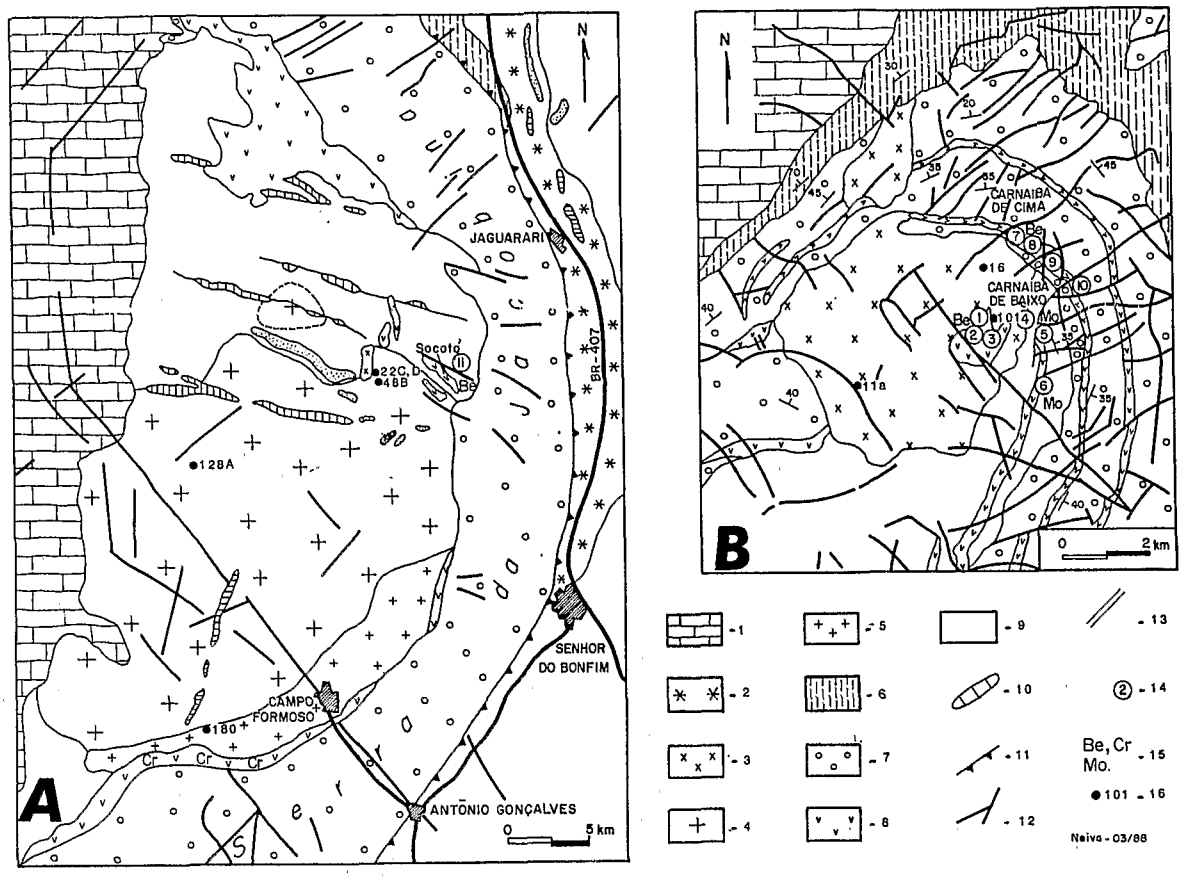

Fig. 2. Geologic sketch maps of the Campo Formoso (2A) and Carnaíba (2B) mining districts. 1=Proterozoic carbonate cover; 2=Jaguarari granitoid; 3=Carnaíba leucogranite; 4=two-mica porphyritic to fine-grained Campo Formoso leucogranite (γ2); 5=two-mica coarse-grained Campo Formoso leucogranite (γ1); 6=chlorite schists; 7=volcanosedimentary formations of the Serra da Jacobina; 8=serpentinites; 9=Archaean gneisses; 10=silicified zones; 11=thrust fault; 12=faults; 13=roads; 14=prospecting pits: 1-Bode, 2-Lagarta, 3-Gavião, 4-Formiga, 5-Braúlia, 6-Marota, 7-Trecho Velho, 8-Trecho Novo, 9-Bica, 10-Cabra, 11-Socotó; 15=Be-green beryl, Cr-chromite, Mo-molybdenite mineralization; 16=analyzed samples from Campo Formoso and Carnaíba granites.

The Be-(Mo-W) mineralization

Emeralds are found in K-metasomatite bodies associated with Transamazonian pegmatites intruding the serpentinite layers. The metasomatic rocks are interpreted as representing the fossil channel-ways of fluid-rock interactions between pegmatitic veins and serpentinites (Rudowski, 1989). Emeralds are intensively exploited in several mining districts known as Carnaíba de cima and Carnaíba de baixo in Carnaíba, and Socotó in Campo Formoso (Fig. 2). In Carnaíba, the emerald-bearing K-metasomatites are developed (i) in roof pendants of serpentinites within the granite, (ii) in imbricated structures within the basement or (iii) within serpentinite-quartzite intercalations of the Jacobina series. In Socotó, the serpentinites appear as imbricated structures on the Archaean gneissic basement (Fig. 2). The mineralized structures reveal the effects of tectonic deformation: crenulation of the metasomatites and boudinage of the emerald-bearing veins are common.

The mineralization is related to intrusive pegmatites crosscutting the serpentinite layers. Both rocks subsequently were pervaded by hydrothermal fluids. The multi-stage infiltration process provoked:

(1) the desilicification and albitization of the pegmatites;
(2) the biotitization of the serpentinites characterized by the formation of monomineralic mica zones developed on the rims of the pegmatitic veins and the so-called K-metasomatites which are composed of pure phlogopite crystals (Rudowski *et al.*, 1987); and,
(3) the deposition of emerald, molybdenite and scheelite within the K-metasomatites and, sometimes, the albitized pegmatites.

PETROGRAPHY, GEOCHEMISTRY AND TRACE ELEMENTS OF THE GRANITES AND ASSOCIATED MINERALIZATIONS

The Campo Formoso and Carnaíba granites

These two-mica granites display similar parageneses and consist of quartz, plagioclase (An_{20} to An_0), micro-

Table 1. Major and trace element contents of the granitic and metasomatic samples from Campo Formoso (CF) and Carnaíba (CA). M=emerald-bearing metasomatites from Socotó (SO) and Carnaíba (CA)

	CF180 γ1	CF48B γ1G	CF128A γ2a	CF22C γ2b	CF22D γ2b	SO1 M	SO13 M	SO100 M
SiO_2 (wt.%)	71.59	71.74	72.29	73.93	73.56	40.57	62.12	42.72
Al_2O_3	15.03	15.33	14.01	14.33	14.42	25.17	12.33	12.35
Fe_2O_3	1.62	1.21	1.58	1.29	1.16	5.50	4.75	10.25
MnO	0.02	0.03	0.02	0.03	0.08	0.04	0.08	0.17
MgO	0.35	0.32	0.29	0.34	0.26	9.98	9.89	20.53
CaO	0.88	0.60	0.96	0.97	0.81	2.16	0.48	1.62
Na_2O	3.40	4.12	3.59	3.97	4.00	2.15	2.08	0.13
K_2O	5.12	4.40	4.94	4.41	4.00	2.81	5.26	8.71
TiO_2	0.17	0.08	0.16	0.12	0.10	0.17	0.11	0.34
P_2O_5	0.28	0.20	0.12	0.16	0.17	0.28	0.16	0.10
I.L.	0.93	0.93	0.54	0.70	0.75	3.47	1.79	1.62
Total	99.39	98.96	98.50	100.25	99.31	92.30	99.05	98.54
Ba (ppm)	496	122	438	366	388	140	199	221
Rb	273	335	288	265	348	214	526	1029
K/Rb	156	109	142	138	95	109	83	70
Sr	143	41	117	135	114	570	142	12
Be	2.5	3.7	1.7	5.09	6.09	58	77	16.5
Sc	4.4	2.5	2.7	2.4	2.2	9.8	6.5	14.3
Co	<5	<5	<5	<5	<5	38	24	48
Cr	11	5	8	9	<5	1761	1678	4050
Ga	29	33	26	23	36	45	32	25
Nb	8	5	7	9	15	<5	6	9
Ni	10	<5	<5	10	20	310	281	624
Th	15	<5	29	19	21	<5	<5	<5
V	23	8	12	6	8	59	31	89
Y	9	9	12	11	15	<5	<5	<5
Zn	50	46	44	51	49	53	44	8
Zr	109	39	146	83	87	9	13	19

	CA16 γCA	CA11a γCA	CA101 γCA	FOR100 M	BO400 M	LA5 M	MA200 M	BO106 M
SiO_2 (wt.%)	73.31	72.93	73.52	42.96	40.39	56.00	41.37	40.39
Al_2O_3	14.51	14.05	14.05	14.86	17.42	15.88	13.01	16.75
Fe_2O_3	1.13	1.48	1.12	7.73	8.19	8.66	10.08	10.96
MnO	0.03	0.03	0.03	0.22	0.17	0.40	0.08	0.56
MgO	0.16	0.32	0.24	21.51	20.70	8.24	21.66	14.66
CaO	0.70	0.96	0.81	0.13		0.29		0.93
Na_2O	3.79	3.59	3.99	0.20	0.16	1.56	0.25	0.13
K_2O	4.82	5.29	4.91	10.33	9.75	7.08	9.21	9.89
TiO_2	0.10	0.16	0.11	0.19	0.08	0.28	0.24	0.28
P_2O_5	0.20	0.15	0.17	0.17	0.08	0.08	0.11	0.68
I.L.	0.60	0.58	0.52	1.54	1.67	1.77	1.23	2.00
Total	99.35	99.54	99.47	99.84	98.61	100.24	97.54	97.23
Ba (ppm)	233	355	255	65	49	142	298	84
Rb	433	361	395	2334	2184	1786	2012	3162
K/Rb	92	122	103	37	37	33	38	26
Sr	65	95	76	13.8	27	43	15	31
Be	10.6	4.5	8.8	24.1	<0.5	16.7	8.39	33.09
Sc	2.7	3	2.5	13.8	8.1	7.59	11.8	5.5
Co	<5	67	100	62	73	37	87	59
Cr	<5	9	6	4631	3243	1937	133	3346
Ga	27	ND	ND	56	25	67	28	55
Nb	19	11	8	53	42	188	43	181
Ni	11	10	13	1237	901	517	682	698
Th	19	24	20	<5	<5	<5	<5	<5
V	6	<5	<5	56	30	30	90	15
Y	9	10	9	<5	<5	<5	<5	5
Zn	55	60	59	479	340	565	134	1456
Zr	89	128	86	18	8	7	65	11

Table 2. CIPW norm of the granitic samples from Campo Formoso and Carnaíba

Vol. %	CF180 γ1	CF48B γ1G	CF128A γ2a	CF22C γ2b	CF22D γ2b	CA16 γCA	CA11A γCA	CA101 γCA
Q	29.82	29.12	29.59	31.19	32.72	31.08	28.97	29.36
Or	30.28	26.03	29.22	26.08	23.66	28.51	31.29	29.04
Ab	28.74	34.82	30.34	33.55	33.81	32.03	30.34	33.72
An	2.54	1.67	3.98	3.77	2.91	2.17	3.79	2.91
Hyp	2.64	2.22	2.45	2.30	2.07	1.69	2.42	1.86
Mt	0.39	0.29	0.38	0.31	0.28	0.27	0.36	0.27
Ilm	0.32	0.15	0.3	0.23	0.19	0.19	0.30	0.21
C	2.95	3.16	1.28	1.63	2.43	2.25	1.01	1.09
Ap	0.61	0.44	0.26	0.35	0.37	0.44	0.33	0.37
An	4.13	2.68	6.27	5.95	4.82	3.46	5.79	4.43
Ab	46.68	55.70	47.75	52.92	55.99	51.08	46.38	51.35
Ov	49.19	41.63	45.98	41.14	39.19	45.46	47.83	44.22
A/CNK	1.59	1.68	1.47	1.53	1.63	1.55	1.42	1.44
Rb/Sr	1.9	8.17	2.46	1.96	3.05	6.66	3.8	5.19
Y+Nb	17	14	29	20	30	28	21	17

cline, chloritized biotite and muscovite. Accessory minerals consist of apatite, zircon, allanite, ilmenite, epidote and magnetite. It must be emphasized that the association magnetite-allanite is a typical feature of γ2 and γCA granites. In all facies, petrographic examination reveals that the biotite was substantially chloritized in γ1 and totally in γ2 and γCA, and transformed to an assemblage of chlorite, K-feldspar, titanite and quartz.

Muscovite is of secondary origin (i.e deuteric-hydrothermal) in all granites. It is abundant in γ1 (10 to 20 modal %) as large megacrysts which contain xenomorphic crystals of biotite and, in γ2, it represents 2 to 3 modal % of the rock. In Carnaíba, the muscovite is often developed on biotite crystals.

Major and trace element concentrations were determined by ICP-AES on representative samples of the granites and emerald-bearing metasomatites (Govindaraju and Chouard, 1976). The data are listed in Table 1. The leucocratic granites of Campo Formoso and Carnaíba possess the characteristics of an evolved silico-alkaline granitic series with SiO_2 > 71%, CaO between 0.6 and 0.9%, and TiO_2 varying between 0.08 and 0.17%. S-type features are represented by muscovite and alumino-silicate minerals, A/CNK ratio > 1.42 and normative corundum > 1.01 (Table 2). A/CNK is high and varies from 1.47 to 1.68 for Campo Formoso, from 1.42 to 1.55 for Carnaíba, whereas normative corundum varies from 1.01 to 3.16, respectively. The high A/CNK ratio and normative corundum partly results from the presence of abundant muscovite. However, the secondary origin of this mineral obliterates in part the original geochemical feature of these granites.

Although the granites show S-type characteristics, the association magnetite-allanite is unusual for such peraluminous, leucocratic series. Cuney *et al.* (1990) interpreted the general occurrence of magnetite, allanite and occasional epidote in these granites as the consequence of high oxygen fugacity conditions during emplacement.

In the A-B diagram of Debon and Lefort (1982), where alumina saturation is plotted against the sum of mafic elements (which in our case represents the sum of biotite + magnetite), the Carnaíba and Campo Formoso granitic suites show typical peraluminous evolutionary trends (Fig. 3A). The evolution from γ1 to γ2 to γCA is characterized by a decrease in the sum of mafic elements. The γ1 and γ2 suites present evolutional trends towards more evolved facies (increase in parameter A and decrease in B). The parameter B appears constant for γCA.

Trace element contents are different for the three suites. Each suite shows a decrease in Sr and an increase of Rb during the evolution whereas Sr (up to 143 ppm) and Ba (up to 496 ppm) contents are rather high. In the Bouseily and El Sokhary diagram (1975; Fig. 3B), the granites show a trend typical of strongly differentiated granites. Be values are low in Campo Formoso granites (up to 6.1 ppm) and higher in the Carnaíba suite (4.5 < γCA < 10.6 ppm). Nb and Y contents are very low (14 < γCF < 30 and 17 < γCA < 28) whereas Rb contents are high. In the Thiéblemont and Cabanis (1990) (Y/44)-(Nb/16)-(Rb/100) diagram (Fig. 3C), the samples plot within the field of granites related to syn-collision tectonic environments; these data are in good agreement with the work of Cuney *et al.* (1990), who proposed the generation of these granites by partial melting of an upper continental crust.

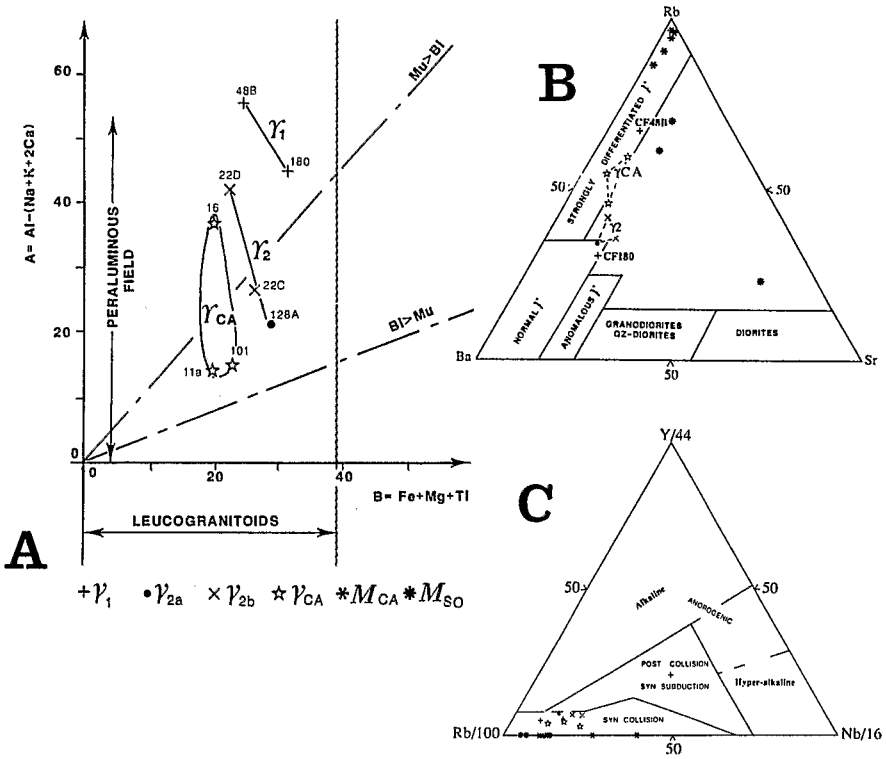

Fig. 3. (A) A-B diagram of Debon and Lefort (1982). Campo Formoso leucogranite: γ1 = two-mica coarse-grained granite; γ2a two-micas fine-grained granite; γ2b = two-mica porphyritic granite; γCA Carnaiba leucogranite; Emerald-bearing metasomatites: MCA=Carnaíba; MSO=Socotó (Campo Formoso). (B) Rb-Ba-Sr diagram of Bouseily and El Sokhary (1975). (C) (Rb/100) - (Y/44) - (Nb/16) diagram of Thiéblemont and Cabanis (1990).

Emerald-bearing K-metasomatites

The K-metasomatites are composed of coarse-grained (size of 1-5 mm up to 1 cm) and fine-grained (size < 0.5 mm) crystals of phlogopite which represent 85 to 99 modal % of the rock. Other minerals consist of apatite (1 to 15 modal % of the rock), sometimes emerald and quartz (< 1% modal). The K-metasomatites are almost pure "phlogopitites" (8.24 < MgO < 21.66%). Relative to the granites, they appear significantly enriched in Cr, Ni, V, Rb, Nb and Be (Table 1 and Fig. 3C). in spite of a scant number of analyses, notably for Campo Formoso, appreciable differences between K-metasomatites of the two districts can be pointed out. For instance, the Carnaíba K-metasomatites have higher enrichments in Rb, Cr, V and Ni than their Campo Formoso counterparts. The preferential enrichment in Rb of Carnaíba K-metasomatites is quantitatively illustrated by the K/Rb ratio, which is consistently very low (26 < K/Rb < 38), whereas the sample SO100 from Campo Formoso gives a K/Rb ratio of 70 for the same K content.

SAMPLES AND ANALYTICAL K-Ar and $^{40}Ar/^{39}Ar$ PROCEDURES

The samples

The conventional K-Ar analyses were performed on mineral separates (biotite, muscovite and phlogopite) from 8 granites and 8 K-metasomatites, and on 3 whole-rock samples from the Carnaíba K-metasomatites. The biotites CF22C, CF22D, CF48B, CF128A, CF180 and the muscovites CF48B and CF180 originate from the Campo Formoso granites; both biotite and muscovite CA11A, CA16, and CA101 are from the Carnaíba granite (Fig. 2). The phlogopites SO1, SO13, and SO100 originate from Socotó. In the Carnaíba massif, five samples of phlogopites were selected: sample MA200 (Marota prospecting pit), FOR100 (Formiga), samples BO106, BO400 (Bode) and LA5 (Lagarta).

The incremental degassing experiments were performed on biotite and muscovite CF180 from Campo Formoso, phlogopite MA200 and emerald CAJ1 from Carnaíba.

$^{40}Ar/^{39}Ar$ analyses were peformed on biotite CF180, muscovite CF180, muscovite CA101 and phlogopite MA200.

The purity of the different separated minerals was checked both under the microscope and by X-Ray diffraction. The biotites from the two granites are affected by an intense chloritization, expressed by a quantity of chlorite varying from 5 to 30% (Tables 3 and 4). All the phlogopites from Socotó and the sample BO400 from Carnaíba are also affected by the chloritization process (Table 4). The Campo Formoso two-mica granites are characterized by a close association of muscovite and minute inclusions of biotite. Biotite-free muscovites were carefully separated prior to K-Ar and $^{40}Ar/^{39}Ar$ dating.

K-Ar dating

K was analyzed by atomic absorption and Ar measured by isotopic dilution, using a ^{38}Ar spike and a modified THN 205 E mass spectrometer (Zimmermann *et al.*, 1985). Six to 15 mg of mineral separates and 10 to 13 mg of rock powder where used for total fusion experiments. The quantity of material used for the experiments was

Table 3. K-Ar contents and ages of the analyzed samples from Campo Formoso

N° Sample	Material	Number of analyses	K average %	^{40}Ar radiogenic average $10^{-6}cm^3.g^{-1}$	^{40}Ar atmospheric average %	Age (±2σ) average Ma
K-Metasomatites						
SO100	Phlogopite + Chlorite (1.5%)	5	7.04	916.9	9.6	1895.0 ± 35.2
SO13 (>1mm)	Phlogopite	4	8.0	1066.4	3.9	1922.4 ± 33.9
SO13 (<1mm)	Phlogopite + Chlorite (1.5%)	2	7.78	1030.6	19.5	1915.0 ± 27.7
SO1 (0.5-0.7mm)	Phlogopite + Chlorite (2%)	3	6.64	914.4	22.1	1961.1 ± 43.2
SO1 (>2mm)	Phlogopite	4	7.76	1134.1	2.7	2032.9 ± 42.4
Granites						
CF22C	Biotite + Chlorite (30%)	3	5.8	764	4.1	1908.4 ± 47.4
CF22D	Biotite + Chlorite (17%)	2	5.2	665.	4.1	1874.9 ± 45.2
CF128A	Biotite	2	5.23	674.1	3.9	1882.9 ± 39.4
CF48B	Biotite	2	6.67	868.6	2.2	1894.9 ± 55.8
	Muscovite	5	7.79	1016.1	4.3	1896.8 ± 33.8
CF180	Biotite + Chlorite (9%)	4	6.18	805.6	7.2	1896.0 ± 23.8
	Muscovite	4	8.31	1221.5	4.7	2040.0 ± 24.2

Table 4. K-Ar contents and ages of the analyzed samples from Carnaíba

N° Sample	Material	Number of analyses	K average %	^{40}Ar radiogenic average $10^{-6}cm^3.g^{-1}$	^{40}Ar atmospheric average %	Age (±2σ) average Ma
K-Metasomatites						
MA200	Phlogopite	12	7.59	1062.4	5.6	1980.6 ± 30.8
	Whole rock	1	7.59	1051.4	2.1	1968.1
FOR100	Phlogopite	5	8.11	1119.7	2.6	1964.2 ± 37.2
	Whole rock	1	8.18	1143.9	2.3	1979.5
BO106	Phlogopite	5	8.30	1143.8	3.4	1962.0 ± 45.9
	Whole rock	1	8.38	1153.0	4.5	1960
BO400	Phlogopite (Chlorite 3%)	7	7.91	1033.4	4.2	1898.7 ± 50
LA5	Phlogopite	4	8.16	1096.2	7.6	1931.6 ± 50.2
Emerald						
CAJ1	Beryl	1	0.0315	323.9	13.7	8180
Granites						
CA16	Biotite + Chlorite (11%)	4	5.81	733.6	4.8	1858.0 ± 31.3
	Muscovite	5	8.53	1175.4	4.2	1961.8 ± 35.6
CA101	Biotite	4	7.6	1024.4	6.3	1935.5 ± 38.2
	Muscovite	8	8.53	1206.7	3.2	1993.4 ± 36.8
CA11A	Biotite + Chlorite (5%)	4	7.12	909.0	4.2	1871.7 ± 49.6
	Muscovite	5	8.25	1142.7	4.5	1968.0 ± 52.3

determined following the potassium concentration of each material.

Incremental gas extraction K-Ar analysis was done by stepwise heating of the samples between 200 and 1300° C (Zimmermann, 1970; 1972). Eight to 11 mg of mica and 45 mg of emerald where used for this purpose. During each step, the temperature of the resistance furnace was held constant for about five hours, thus assuring an equilibrium pressure of the released gases. During each step the extracted gases were transferred to a purification line and ^{38}Ar spike was added. For each sample an integrated age was calculated by summing the $^{40}Ar^*$ liberated at each step and using the total K content of the sample. The error on the individual ages are quoted at 2σ level and were calculated following the statistical analysis of Cox and Dalrymple (1967). Weighted mean ages and corresponding errors were also calculated for selected samples.

$^{40}Ar/^{39}Ar$ experiments

The $^{40}Ar/^{39}Ar$ experimental techniques, described elsewhere (Montigny *et al.*, 1988), are similar to those of Féraud *et al.* (1982; 1986) and Maluski (1985). The samples were sealed in quartz vials and irradiated for 31 hours in the Osiris reactor at the C.E.N. (Saclay, France). The integrated flux was about 5×10^{18} neutrons cm^{-2}. The samples were positioned within the irradiation can at two levels and one monitor was irradiated at each level. A 5.5% variation in the $^{40}Ar^*/^{39}Ar$ ratio for the monitors between the two levels was observed. CaF_2 and K_2SO_4 samples were included in the irradiation package in order to determine the correction factors for interfering isotopes produced by nuclear reactions during irradiation. Measurements of two irradiated salts yielded the following correction factors: $(^{40}Ar/^{39}Ar) = 2.77\times10^{-2} \pm 1.1\times10^{-3}$; $(^{36}Ar/^{37}Ar)Ca = 3.78\times10^{-4} \pm 3.0\times10^{-5}$ and $(^{39}Ar/^{37}Ar)Ca = 7.45\times10^{-4} \pm 3\times10^{-5}$.

Standard hornblende Caplongue (344.5±3.5 Ma; Maluski and Monié, 1988) was used as the flux monitor. The errors, quoted at 1σ in the table and at 2σ in the text, were calculated following the procedure given by Albarède (1976). The formula corresponding to (σ_t is that of Berger and York (1970), which incorporates the error in the $^{40}Ar^*/^{39}Ar_K$ ratio of the monitor but not the error in its age. Therefore, the error of integrated ages includes the error in the irradiated monitor age ($\pm1\sigma$).

K-Ar age determinations

1) Granites

Campo Formoso: The biotites yield ages between 1875 ± 45 Ma and 1908 ± 47 Ma (2σ). The muscovites CF48B and CF180 yield ages of 1897 ± 34 and 2040 ± 24 Ma (2σ), respectively. The biotite-muscovite pair from CF48B sample indicates comparable ages at 1895 ± 56 Ma and 1897 ± 34 Ma, respectively (Table 3). The mean age of two representative samples of the Campo Formoso $\gamma1$ series (biotites CF180 and CF48B) is 1896 ± 22 Ma and the samples of $\gamma2$ series (Obiotites CF128A, CF22C, CF22D) give a mean age of 1888 ± 25 Ma.

Carnaíba. The biotites yield ages between 1859 ± 31 Ma and 1935 ± 38 Ma (2σ). The muscovites from the same samples yield older ages between 1962 ± 35 Ma and 1993 ± 36 Ma (Table 4).

Plotted in a $^{40}Ar/^{36}Ar$ f $^{40}K/^{36}Ar$ diagram (McDougall *et al.*, 1969), the biotites and the muscovites fit isochrons with ages of 1888 ± 32 (MSWD = 1.78; initial $^{40}K/^{36}Ar$ ratio = 295.6 ± 6) and 1979 ± 28 Ma (MSWD = 2.31 ± 6; initial $^{40}K/^{36}Ar$ ratio= 293.5 ± 6), respectively (Fig. 4A and B).

2) K-Metasomatites

Carnaíba: the metasomatites yield whole rock and separated phlogopite ages between 1981 ± 31 Ma (sample MA200, unchloritized) and 1899 ± 50 Ma (sample BO400, chloritized), thus ranging within the 2σ error bar of individual samples (Table 4). With the exception of sample BO400 which contains 3% chlorite, the phlogopites fit an isochron age of 1973 ± 20 Ma (Fig. 4C; MSWD= 5.31, initial $^{40}Ar/^{36}Ar$ ratio = 294.5 ± 5.6) and a weighted mean age of 1965 ± 19 Ma (2σ).

Campo Formoso (Socotó): the metasomatites yield ages between 2033 ± 42 Ma (biot. SO1, unchloritized, $\emptyset$ > 2mm) and 1895 ± 35 Ma (biot. SO100, 1.5% chlorite). All the micas give an isochron age of 1954 ± 30 Ma (Fig. 4D; MSWD = 2.7, initial ratio = 292 ± 5).

Incremental step heating on emerald and mica

Carnaíba Emerald: as expected, emerald contains significant amounts of extraneous argon (Leutwein and Kaplan, 1963), giving an apparent age of 8180 Ma. This unreal age results from the important quantity of radiogenic $^{40}Ar^*$ released by the sample during the step heating ($Q = 323.87\ 10^{-6}\ cm^3.g^{-1}$) and the relatively low K-content of the mineral (K= 0.0315%). Moreover, the degassing spectrum (Fig. 5A), characterized by a strong degassing at 1025° C, indicates that argon is situated within the mineral structure and not on the surface. This experiment is in agreement with the observation of Damon and Kulp (1958), indicating that the ring structure of beryl is prone to trap rare gas.

Micas:

(1) phlogopite from the K-metasomatites and biotite from the granites exhibit very distinct argon release patterns.

The phlogopite MA200 displays its first noticeable $^{40}Ar^*$ release at 820° C, a main pulse of argon degassing at 1025° C and a third pulse at 1280° C (Fig. 5B); this pattern corresponds to the typical argon liberation from phlogopite (Zimmermann, 1970; 1972). The integrated age calculated from a knowledge of the total $^{40}Ar^*$ release ($Q = 1047.82\ 10^{-6}\ cm^3.g^{-1}$) and the K content of the phlogopite (K= 7.59%, Table 4), is 1964 ± 16 Ma.

The biotite CF180 shows a degassing histogram scattered between 620° C and 1300° C with a main argon release between 820° and 1020° C (Fig. 5C). This histogram conforms strictly to the model proposed by Zimmermann (1972), where the pulses of argon release in biotite are viewed as accompanying dehydroxylation processes.

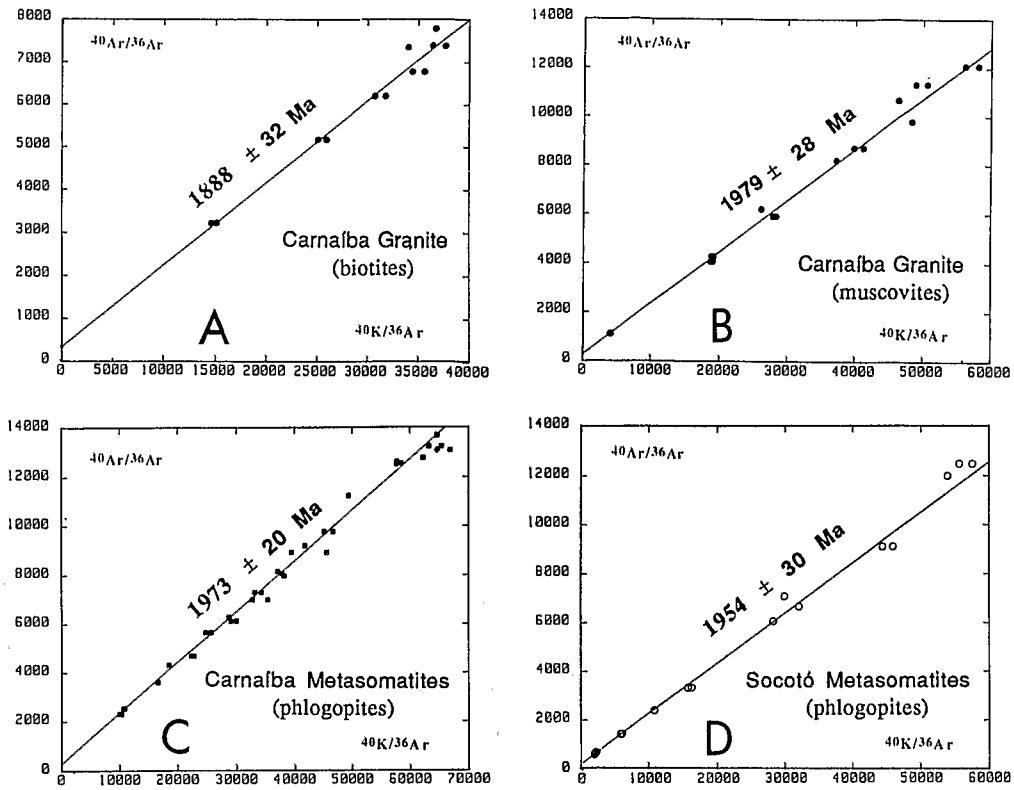

Fig. 4. The $^{40}Ar/^{36}Ar$ versus $^{40}K/^{36}Ar$ isochrons for the biotites and muscovites of Carnaíba granite (A and B) and the phlogopites of Carnaíba and Socotó emerald-bearing K-metasomatites (C and D).

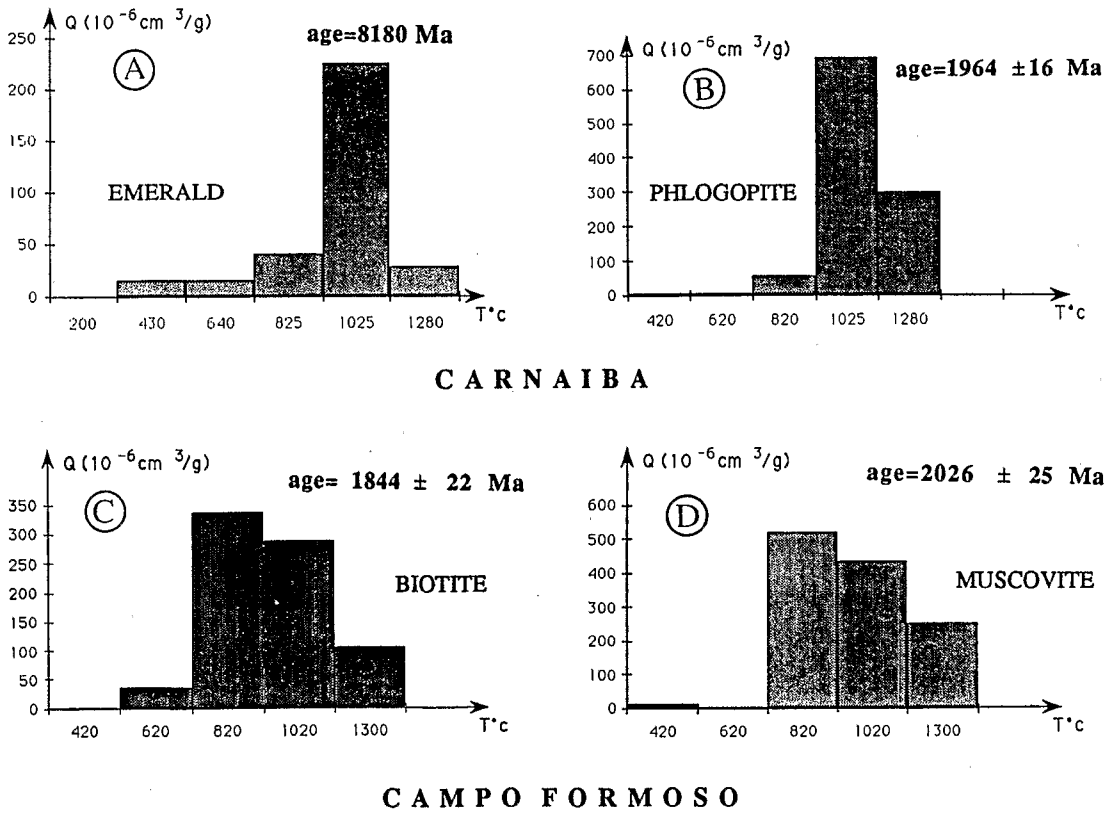

Fig. 5. (A) Measurement by incremental step heating of radiogenic argon held by an emerald from Carnaíba (sample CAJ1); (B) the phlogopite of a K-metasomatite from Carnaíba (sample MA200); (C, D) the couple biotite-muscovite from γ1 Campo Formoso granite (sample CF180). T=temperature (°C). Q=quantity of $^{40}Ar^*$ radiogenic released for each heating step of the sample (10^{-6} $cm^3.g^{-1}$); for all steps, total quantity for each sample is: Q (CAJ1)=323.87 10^{-6} $cm^3.g^{-1}$; Q(MA200)=1047.82 10^{-6} $cm^3.g^{-1}$; Q(Biotite CF180)=769.69 10^{-6} $cm^3.g^{-1}$; Q(muscovite CF180)=1207.76 10^{-6} $cm^3.g^{-1}$. The K content of each mineral is: K(CaJ1)=0.0315%; K(MA200)=7.59%; K(biot. CF180)=6.18% and K(musc. CF180)= 8.31%.

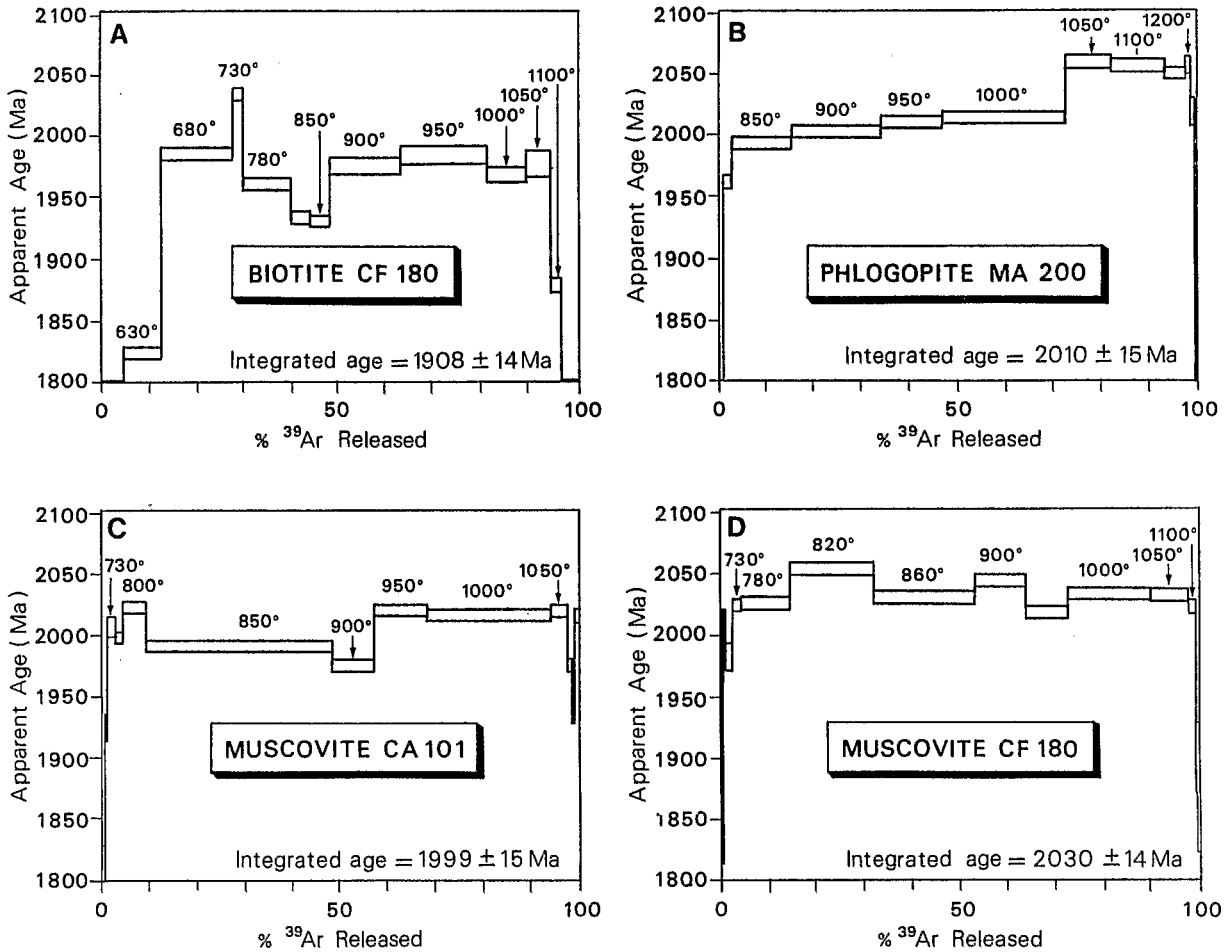

Fig. 6. $^{40}Ar/^{39}Ar$ spectra of the pair biotite (A)-muscovite (D) from γ1 Campo Formoso granite (sample CF180), the muscovite of Carnaíba granite (C) and the phlogopite (B) of Carnaíba metasomatite (sample MA200). The errors are quoted at ± 1σ. in the integrated age, the error in the age of Caplongue hornblende is taken into account.

The total $^{40}Ar^*$ release defines an integrated age of 1844 ± 22 Ma.

(2) muscovite from the Campo Formoso granite exhibits the same argon release pattern of coexisting biotite.

The histogram of argon released from muscovite CF180 (Fig. 5D) shows a first noticeable $^{40}Ar^*$ release at 420° C which is probably associated with the release of hydration water under vacuum within the sheet structure of the mica (Zimmermann, 1970, 1972). The main $^{40}Ar^*$ release begins at the 820° C temperature step and is similar to that obtained for other muscovites (Zimmermann, op. cit.). The calculated age for the muscovite, integrating all the steps is 2026 Ma ± 25 Ma (Q = 1207.76 10^{-6} $cm^3.g^{-1}$; K= 8.31%). The radiogenic argon extracted at 420° C represents only 0.84% of the whole radiogenic argon released by the mineral; if this argon were inherited argon, the age of the sample would be 2016 Ma.

$^{40}Ar/^{39}Ar$ data

The four $^{40}Ar/^{39}Ar$ release spectra obtained on phlogopite, biotite and muscovite (Fig. 6) from Carnaíba and Campo Formoso show noticeable disturbances without any plateau age:

(1) the biotite CF180 (Fig. 6A) yields the most disturbed spectrum with an integrated age of 1908 ± 14 Ma (2σ) (Table 5B). This spectrum is characterized by

- (a) a sharp increase of ages (from 715 to 2032 Ma) at low temperature steps (450° to 730° C) followed by
- (b) a decrease until 850° C, giving a general humped shape for these two first sections;
- (c) a flat segment that appears between 900° and 1050° C corresponding to 46.3% of the total $^{39}Ar_K$ released with concordant ages, therefore defining an integrated age of 1973 ± 14 Ma (2σ); and
- (d) the end of the spectrum corresponds to a sharp decrease of ages (from 1877 to 1752 Ma) for the 1100-1500° C temperature steps.

(2) the phlogopite MA200 from Carnaíba yields a staircase release spectrum (Fig. 6B) with apparent ages increasing with temperature (Table 5A). Two segments can be defined on this spectrum: the first

Table 5A. Results of $^{40}Ar/^{39}Ar$ measurements obtained on the samples from Carnaíba. The error quoted at ± 1σ in the integrated age takes into account the error in the age of Caplongue hornblende standard

Step T(°C)	100 x $^{40}Ar^*$ / Total ^{40}Ar	^{39}Ar / $\Sigma(^{39}Ar)$	$^{37}Ar_{Ca}$ / $^{39}Ar_k$	$^{40}Ar^*$ / $^{39}Ar_k$	Apparent age	SD (1 σ)
MA 200, Phlogopite (metasomatite)						
J = 0,0088018						
630	68.8	0.002	0	69.33	859	82
680	65.3	0.002	0	156.41	1562	48
740	87.6	0.006	0	189.17	1768	16
800	82.6	0.019	0	223.06	1960	6
850	99.3	0.126	0	228.90	1991	5
900	99.4	0.188	0	230.83	2001	5
950	99.7	0.126	0	232.17	2008	5
1000	99.6	0.259	0	232.69	2011	5
1050	99.5	0.095	0	241.33	2055	5
1100	99.1	0.113	0	240.80	2052	5
1150	99.0	0.038	0	239.50	2046	5
1200	94.1	0.016	0	241.09	2054	7
1300	94.7	0.008	0	233.76	2016	12
1500	28.1	0.002	0	197.53	1818	27
Integrated age : 2010 ± 15 Ma						

Step T(°C)	100x $^{40}Ar^*$ / Total ^{40}Ar	^{39}Ar / $\Sigma(^{39}Ar)$	$^{37}Ar_{Ca}$ / $^{39}Ar_k$	$^{40}Ar^*$ / 39Ar_k	Apparent age	SD (1 σ)
CA 101 Muscovite (granite)						
J = 0,0083210						
550	71.2	0.002	0	130.60	1327	95
630	68.9	0.003	0	208.23	1814	14
680	93.7	0.005	0	229.07	1925	11
730	93.6	0.014	0	245.12	2006	8
765	96.4	0.018	0	243.35	1997	5
800	97.7	0.047	0	248.17	2021	5
850	99.6	0.391	0	241.94	1990	5
900	99.0	0.091	0	238.73	1974	5
950	99.7	0.110	0	247.79	2019	5
1000	99.7	0.255	0	247.10	2015	5
1050	99.3	0.036	0	247.69	2018	5
1100	96.9	0.012	0	238.77	1974	6
1200	91.4	0.004	0	231.85	1939	14
1500	85.5	0.012	0	246.72	2014	6
Integrated age : 1999 ± 15 Ma						

+ The error on the mean age takes into account the error on the standard40

Table 5B. Results of 40Ar/39Ar measurements obtained on the samples from Campo Formoso. The decay constants recommended by Seiger and Jäger (1977) were used

Step T (°C)	100x $^{40}Ar^*$ / Total ^{40}Ar	^{39}Ar / $\Sigma(^{39}Ar)$	$^{37}Ar_{Ca}$ / $^{39}Ar_k$	$^{40}Ar^*$ / $^{39}Ar_k$	Apparent age	SD (±1σ)
CF 180 Muscovite (granite)						
J = 0,0083210						
450	57.6	0.001	0	138.64	1384	16
550	54.0	0.003	0	211.31	1830	17
630	90.8	0.006	0	246.28	2011	8
680	85.5	0.013	0	240.07	1981	11
730	95.7	0.019	0	248.70	2023	5
780	98.1	0.103	0	248.87	2024	5
820	99.4	0.177	0	254.69	2052	5
860	95.2	0.211	0	249.71	2028	5
900	99.6	0.107	0	252.26	2041	5
950	98.1	0.086	0	247.07	2015	5
1000	99.7	0.175	0	250.19	2030	5
1050	99.7	0.081	0	249.59	2028	5
1100	97.3	0.013	0	247.80	2019	6
1200	77.5	0.002	0	223.80	1897	29
1450	64.8	<0.001	0	216.30	1857	38
Integrated age : 2030 ± 14 Ma						

Step T (°C)	100x $^{40}Ar^*$ / Total ^{40}Ar	^{39}Ar / $\Sigma(^{39}Ar)$	$^{37}Ar_{Ca}$ / $^{39}Ar_k$	$^{40}Ar^*$ / $^{39}Ar_k$	Apparent age	SD (±1σ)
CF 180 Biotite (granite)						
J = 0.0088018						
450	83.0	0.011	0.1319	55.21	715	14
550	96.6	0.035	0.0315	114.03	1254	5
630	99.4	0.077	0	198.54	1823	5
680	99.7	0.152	0	227.33	1983	5
730	99.9	0.021	0	236.78	2032	5
780	99.7	0.101	0.0162	222.66	1958	5
820	99.3	0.043	0.0333	217.80	1931	5
850	99.4	0.041	0.0333	217.39	1929	5
900	69.4	0.149	0.0312	225.47	1973	7
950	71.6	0.179	0.0211	227.17	1982	7
1000	98.5	0.084	0.0462	224.15	1966	6
1050	28.5	0.051	0.0654	225.68	1974	10
1100	98.7	0.022	0.0731	208.02	1877	6
1200	1.8	0.020	0.2225	85.65	1014	105
1500	33.6	0.013	0.3458	186.35	1752	12
Integrated age : 1908 ± 14 Ma						

segment is comprised between 850° and 1000° C and yields an integrated age of 2002 ±16 Ma (2σ) corresponding to 62.5% of the total $^{39}Ar_K$ released; the second segment, between 1050° and 1200° C, corresponds to 26.2% of the total $^{39}Ar_K$ released and defines an integrated age of 2052 ± 10 Ma (2σ).

(3) the muscovite CA101 yields three consecutive segments (Fig. 6C):

(a) a humped shape from 550° to 900° C,

(b) a flat segment with concordant ages between 950° and 1050° C corresponding to 40.1% of the total $^{39}Ar_K$ released, and giving an integrated age of 2016 ± 10 Ma (2σ), and

(c) a highly disturbed section (but only involving about 3% of the argon) from 1100° to 1500° C.

For the intervals (a) and (b), we observe a standard deviation of 47 Ma (apparent age difference between the 800° and 900° C steps) corresponding to a 2.4% deviation relative to the integrated age.

(4) the muscovite CF180 yields a less disturbed spectrum (Fig. 6D), characterized by an integrated age of 2032 ±10 Ma(2σ) corresponding to the interval between the 730-1100° C steps, i.e 97.2% of the total $^{39}Ar_K$. The standard deviation, calculated between the lowest and highest apparent ages corresponding to the 820° and 950° C steps, is 1.6% for an integrated value of 2032 Ma.

DISCUSSION

K-Ar determinations on granites reveal the following features:

- The age of muscovite exceeds that of coexisting biotite by about 100 to 150 Ma, as for muscovites and biotites from the Carnaíba granite which yield age clusters of 1979 ± 28 and 1888 ± 32 Ma (2σ), respectively (Fig. 4). Moreover, biotites from the two granites yield ages that are indistinguishable: they cluster around an average value of 1890 ± 30 Ma. The difference in age between muscovite and biotite can be related to the presence of chlorite within biotite and its consecutive decrease in K% content. In fact, inspection of K content of biotite (Tables 3 and 4) shows that the lower ages are related to a lower K concentration of the mineral.

- The muscovite CF48B from Campo Formoso granite gives the same age as the associated biotite (1895 Ma; Table 3). This could be due partly to the presence of minute chloritized-biotite inclusions within the muscovite separates. In fact, the K content (K = 7.79%) of this muscovite is lower than the K content of the other muscovites (K > 8.25%; Tables 3 and 4).

- The conventional K-Ar age of muscovite CF180 from the Campo Formoso intrusive, 2040 ± 24 Ma, falls in the same range as those defined by step heating, 2026 ± 25 Ma and $^{40}Ar/^{39}Ar$, 2030 ± 14 Ma (Fig. 6D). Incremental step heating shows that 99% of the radiogenic argon is released after the 820° C step, thus implying that it is located within the crystal structure of the mica (Fig. 5D) and therefore not inherited. Consequently, the K-Ar age obtained on muscovite CF180 (2040 ± 24 Ma) represents a good estimate of the crystallization age of the γ1 Campo Formoso intrusive series. This age is definitely outside the age range defined by muscovites from Carnaíba (1973 ± 28 Ma).

K-Ar determinations on emerald-bearing K-metasomatites from the two mining districts exhibit the same pattern and spread between 1900 and 2000 Ma. It should be noted that phlogopites from the Carnaíba area (Table 4) are richer in K and poorer in chlorite than those from Campo Formoso, and display higher apparent ages.

The age obtained on SO1 (2033 ± 42 Ma; grain-size > 2mm, K = 7.76%, Table 3) is slightly higher than the ages obtained on Campo Formoso K-metasomatites. For this sample, the phlogopite with a grain-size between 0.5 and 0.7 mm, is intensely affected by chloritization (K = 6.64%) and yields an age of 1961 ± 43 Ma. The difference in radiogenic argon between the youngest and oldest phlogopites, is around of 20% of the total argon retained by the oldest sample.

These results lead to four possible interpretations:

(a) crystallization of two distinct generations of phlogopite in the same rock and at different times;

(b) phlogopite suffered a remobilization event after its crystallization, resulting in argon loss and chloritization; in this case, the calculated age has no significance;

(c) phlogopite released radiogenic argon in the fluid phase, part of which may have been captured by coeval emerald. Following this interpretation, the radiogenic argon contained within the emerald on a per gram basis, corresponds to 31% of the argon retained by phlogopite, comparing the step heating release of emerald CAJ1 (Fig. 5A) and phlogopite MA200 (Fig. 5B); or

(d) emerald incorporated its argon from the fluid when it initially crystallized independant of capturing argon subsequently released by phlogopite. Considering that emerald and phlogopite belong to the same metasomatic rock and crystallized from the same hydrothermal fluid, (a) appears not probable but (b), (c) and (d) are likely.

The integrated $^{40}Ar/^{39}Ar$ ages (Table 5) agree well with conventional K-Ar ages. K-Ar and integrated $^{40}Ar/^{39}Ar$ ages are respectively: 1896 ± 24 and 1908 ± 28 Ma (2σ) (Fig. 6A) for biotite CF180, 2040 ± 24 Ma and 2030 ± 28 Ma (Fig. 6B) for muscovite CF180, 1993 ± 37 and 1999 ± 30 Ma (Fig. 6C) for muscovite CA1 01, and 1981 ± 31 and 2010 ± 30 Ma (Fig. 6D) for phlogopite MA200. Therefore,

we can state that the neutron irradiation did not provoke any significant loss of Ar-induced isotopes (Hess and Lippolt, 1986).

The four $^{40}Ar/^{39}Ar$ spectra can be discussed as follows:

(a) the humped shape spectrum of biotite CF180 exhibits a pattern of chloritized biotite (Hess *et al.*, 1987) marked by a saddle between the interval 730° and 900° C which can be interpreted as a recoil effect of ^{39}Ar from biotite to chlorite during the irradiation (Lo and Onstott, 1989; Ruffet *et al.*, 1991). In fact, CF180 biotite contains about 9% chlorite (Table 3); the general disturbed aspect of the spectrum is thus due to differential thermal release of argon from each mineral with variable $^{40}Ar/^{39}Ar$ ratios. The same sample yields ages of 1844 ± 22 Ma and 1896 ± 24 Ma by integrated K-Ar step heating and conventional K-Ar respectively. Therefore, the age of 1973 ± 14 Ma calculated on the flat segment of the $^{40}Ar/^{39}Ar$ spectrum (steps 900-1050° C) with only 46.3% of the total $^{39}Ar_K$ released from biotite CF180 cannot be interpreted as a plateau age;

(b) the two $^{40}Ar/^{39}Ar$ spectra MA200 and CA101 present decreasing perturbations as revealed by the decrease of 3.1 and 2.4% respectively, of the maximum deviation between steps calculated on the different flat portions of the spectra. The integrated age calculated on phlogopite MA200 between the segments 850° and 1200° C, (2016 ±10 Ma), cannot be considered as a plateau age due to a probable partial loss of radiogenic argon as revealed by the staircase aspect of the spectrum;

(c) the less disturbed spectrum represented by the muscovite CF180 yields a maximum deviation of 1.6% for the 730-1100° C steps and the highest $^{40}Ar/^{39}Ar$ integrated age, i.e 2032 ± 1 0 Ma (2σ). We consider that this age represents the best estimation of the crystallization age of sample CF180. The lack of a high amount of radiogenic argon released at low or high temperature during the incremental step heating K-Ar and $^{40}Ar/^{39}Ar$ experiments (Figs. 5 and 6), suggests that excess argon cannot be viewed as responsible for the relatively higher ages obtained on the muscovite CF180.

In conclusion, we may emphasize several characteristics of the K-Ar and $^{40}Ar/^{39}Ar$ results:

- biotite from granites and phlogopite from metasomatites without well defined plateau, yield distinct ages characterized by representative data around 1900 Ma for biotite, and a spread between 1900 and 2000 Ma for phlogopite. The isochron age of 1973 ± 20 Ma calculated for the unchloritized metasomatites of Carnaíba represents the best estimate crystallization age.
- for biotite, and to a lesser extent for phlogopite, the lowest ages are given by chloritized minerals. For muscovite, the same conclusion can be drawn when comparing pure muscovites to biotite-bearing muscovites as shown by the sample CF48B. Therefore, the 1979 ± 28 Ma isochron age obtained on the biotite-free muscovites of the Carnaíba granite can be considered as the crystallization age of this mineral.

on the basis of conventional K-Ar, $^{40}Ar/^{39}Ar$ and K-Ar step heating data, a crystallization age of 2032 ± 10 Ma is proposed for the muscovite CF180 from the γ1 Campo Formoso granite.

GEOLOGICAL SIGNIFICANCE OF THE K-Ar AND $^{40}Ar/^{39}Ar$ AGES

The K-Ar apparent ages, which spread within a wide range between 1860 Ma and 2040 Ma, and the complex $^{40}Ar/^{39}Ar$ degassing spectra of the micas reflect a subsequent disturbance and reopening of the K-Ar system. This pervasive alteration affected both granites and metasomatites due to a thermal overprint younger than the granitic emplacement. Geological evidences lead to the conclusion that a deformational event occurred after the granitic emplacement. For example, emerald mineralization contained in serpentinites exhibits isoclinal folding with boudinage and crenulation. In Socotó, the mineralized serpentinites occur as imbricated structures on the Archaean gneissic basement (Rudowski *et al.*, 1987). The phlogopitites are chloritized, displaying the lowest K-Ar ages (1895 ± 35 Ma). Therefore, it is likely that the thermal overprint mirrors the deformational event, giving rise to the partial reopening of the K-Ar clock of some of the micas and consequently their younger ages.

Chloritization of biotite appears to be a good indicator of this post-crystallization effect. Higher degrees of secondary alteration result in higher amounts of radiogenic Ar loss, resulting in younger ages. However, as stated before, a maximum standard deviation of only 182 Ma (10%) is observed for entire set of K-Ar and $^{40}Ar/^{39}Ar$ integrated ages, thus reflecting rather low radiogenic Ar losses, overall.

For Campo Formoso, these radiogenic Ar losses might explain:

(1) the low K-Ar ages obtained on biotites from γ1 and γ2 granitic intrusives;

(2) the relatively small difference between the Rb/Sr ages (Fig. 7) previously reported by Torquato *et al.* (1978) for the γ1 granite (1978 ± 24 Ma), the 1969 ± 29 Ma proposed by Sabaté *et al.* (1990) integrating the γ1 and γ2 granitic units, and the proposed 2032 ± 10 Ma age of this study for the crystallization of muscovite of the γ1 granite;

(3) the large variation (1895 to 2033 Ma) obtained for the emerald-bearing phlogopitites of Socotó. These phlogopites yield a mean age of 1954 ± 30 Ma which, considering the degree of chloritization of this phase, might represent a minimum age of crystallization for these metasomatites. Though the age assignments are generally good, this disturbance makes it difficult to assess a precise age for

the emerald formation of Socotó and also to assign an age relationship between γ1 or γ2 intrusives and the related emerald mineralization.

For Carnaíba, the K-Ar ages obtained on biotites (1888 ± 32 Ma) and the Rb/Sr ages measured on whole rock samples (1883 ± 87 Ma with MSWD = 0.8; Sabaté *et al.*, 1990) reflect the high degree of alteration of the different phases and emphasize the importance of the chloritization process. These ages cannot be considered as crystallization ages of the Carnaíba granite. The K-Ar data obtained on coexisting muscovites which are free of inclusions of biotite fit an isochron with an age of 1979 ± 28 Ma which must reflect the time of the deuteric hydrothermal muscovitization. Meanwhile, $^{40}Ar/^{39}Ar$ spectrum of muscovite CA101 exhibits argon perturbations without any plateau age (integrated age of 1999 ± 30 Ma) showing that this muscovite was also affected by an hydrothermal overprint. The effect of hydrothermal alteration on the muscovite K-Ar clock is less documented than for biotite or phlogopite (Harrison *et al.*, 1985). Nevertheless, Hess *et al.* (1987) observed that hydrothermal heating of muscovite with an originally well-defined plateau causes negligible loss of argon but induces moderate discordancies in the release spectrum. Thus, the K-Ar isochron age of 1979 ± 28 Ma of the Carnaíba muscovites might be considered as a representative age for the muscovitization process. This process, related to a pervasive subsolidus alteration, therefore developed at a high geothermal temperature (500-600° C) which was obtained during deuteric cooling of the pluton after its emplacement. Since the closure temperature of muscovite (350-375° C, Dodson, 1973; Dunlap *et al.*, 1991) and biotite (300-325° C, Berger and York, 1981) are different, the age of muscovite is slightly older than biotite. However, the closure temperatures are of the same order of magnitude, and the cooling ages of magmatic biotite and deuteric muscovite are not greatly separated in time. Therefore, the 1979 ± 28 Ma age obtained by K-Ar on the muscovites represents the best estimate of the Carnaíba granite cooling age.

Considering the K-Ar data obtained on the Carnaíba metasomatites, 1958 ± 45 Ma (all the data) and 1973 ± 20 Ma (excluding the chloritized sample BO400), we suggest that the mineralization and the metasomatic process affecting the granitic country rocks is contemporaneous with the deuteric-hydrothermal muscovitization evidenced in these granites.

The petrography of the Carnaíba granite showed that this pluton displays mineral parageneses similar to those found in the Campo Formoso pluton. Chemically, all the granitic facies are peraluminous. The composite Campo Formoso pluton has a wide degree of differentiation whereas the Carnaíba pluton is more homogeneous. These differences in the chemical trends are assumed to have resulted from the heterogeneity of the source material of the parent magma (Rudowski, 1989; Cuney *et al.*, 1990). The radiometric data obtained in this study yield different cooling ages for the Carnaíba granite, i.e 1979 ± 28 Ma, and for the first granitic intrusive unit of Campo Formoso, i.e 2032 ± 10 Ma. These granites were emplaced during the Transamazonian orogeny but the gap in time suggested here for the emplacement of these two granitic series per-

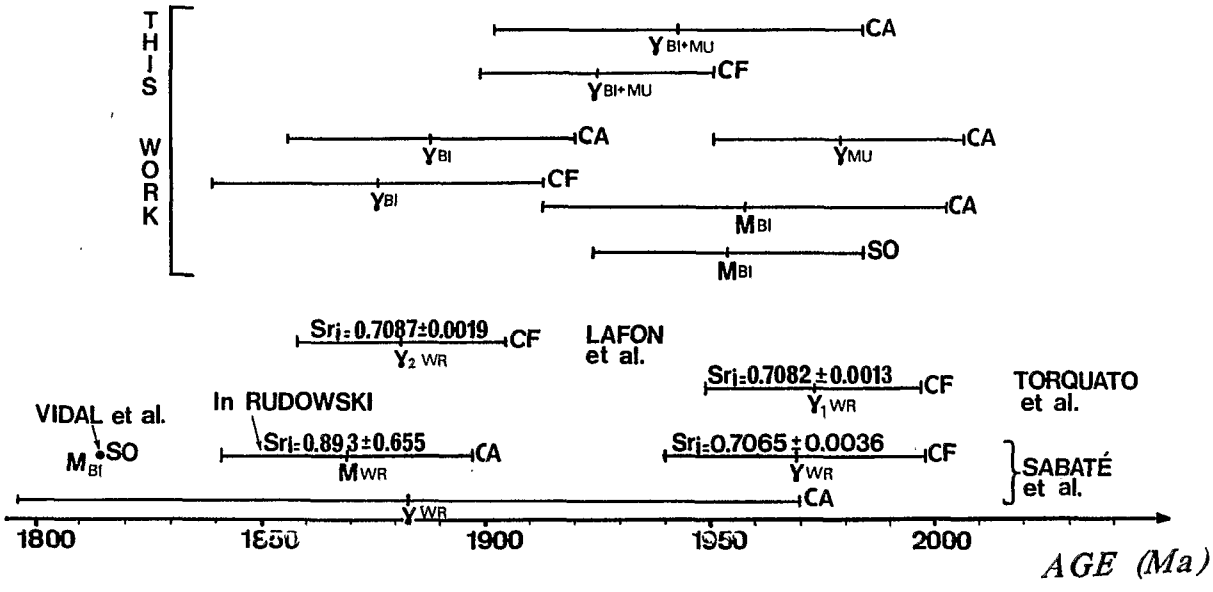

Fig. 7. Compilation of radiometric data obtained on Carnaíba (CA) and Campo Formoso (CF) granites (γ) and associated emerald-bearing metasomatites (M). Rb/Sr-Torquato *et al.* (1978), Lafon (1988), Rudowski (1989), Sabaté *et al.* (1990) and Vidal *et al.* (1992). K/Ar-this work; BI=biotite; MU=muscovite; WR=whole rock; Sri=initial strontium ratio. SO= Socotó emerald deposit.

mits a different source region of melting within the continental crustal section for the two peraluminous granites.

METALLOGENIC CONSEQUENCES

The close time relationships between granite emplacement, deuteric muscovitization and emerald crystallization in K-metasomatitic country-rocks has long been recognized (Beus, 1966). In that sense, the age pattern obtained for the Carnaíba emerald district would suggest a similar but more general genetic model as proposed by Scherba (1970), for Sn-W-Mo-Be mineralization related to acid magmatism. In that model, metasomatism not only affects the apical part of the granitic cupola, giving rise to muscovitization and greisenization, but also develops alteration halos and mineralization through fluid infiltration into the country-rock. In the case of the Brazilian granite-related emerald deposits, the emerald-bearing K-metasomatites result from a fluid infiltration process by percolation along the preexisting pegmatites and adjacent serpentinites (Giuliani and Couto, 1988). The origin of this fluid is unknown, but the muscovitizing fluids could be a good candidate.

A great proportion of the ages deduced from K-Ar and Rb-Sr measurements on micas from the granites and metasomatites are younger than the best estimate of the cooling ages of γ1 Campo Formoso granitic unit (2032 Ma) and Carnaíba granite (1979 Ma). This clearly results from the secondary thermal overprint affecting both radiogenic systems accompanied by isoclinal folding, boudinage and crenulation of the emerald-bearing K-metasomatites. The question arises whether the age of this remobilization can be estimated or not. Two hypotheses can be proposed:

(1) the overprint resulted from a much younger event at relatively low temperature which accounts for the slight argon loss reflected by the $^{40}Ar/^{39}Ar$ step heating spectra. This event could be represented by the Braziliano orogenic phase dated in Bahia State at 700-500 Ma (Moutinho da Costa and Mascarenhas, 1982). However, structural evidence is lacking in the Serra de Jacobina belt to support this hypothesis (McReath and Sabaté, 1987);

(2) a second possibility is to relate this thermal overprint to late stage activity of the tectonothermal Transamazonian event which is dated in the São Francisco craton at 2200-1800 Ma (Brito Neves *et al.*, 1980; Romano *et al.*, 1991) as evidenced in the study area (McReath and Sabaté, 1987; Bertrand and Jardim de Sã, 1990). Following this hypothesis, the granites and their accompanying deuteric-hydrothermal systems related to the emerald metasomatites could be considered as having developed during a late phase of Transamazonian magmatism followed shortly after by a deformational compressive phase of the same orogeny. A mean age of 1890 ± 30 Ma (2σ), calculated using the whole set of K-Ar and $^{40}Ar/^{39}Ar$ ages from the biotites of Campo Formoso and Carnaíba granites may tentatively be assigned to this overprint, assuming that a tight cluster of K-Ar ages, as that defined by biotites from the two granites, should have a geological significance. Nevertheless, the K-metasomatites from Socotó which are also affected by this chloritization, yield an older mean age of 1954 ± 30 Ma. The Rb-Sr age distribution obtained on the granites and K-metasomatites (Fig. 7) show also a great variation, with ages of 1814 Ma for the phlogopites of Socotó (Vidal *et al.*, 1992) and 1869 ± 28 Ma for the phlogopites of Carnaíba (in Rudowski, 1989). The important discrepancy between these data and the present K-Ar and $^{40}Ar/^{39}Ar$ determinations for equivalent samples, may be related to the degree of chloritization of each sample. Therefore, we cannot assign a mean age for the tectonothermal overprinting that affected both biotite and phlogopite.

Due to the lack of structural evidence for a Braziliano event (700-500 Ma) in this region, we propose a late stage Transamazonian age for the thermal overprint provoking the chloritization of the Transamazonian granites and metasomatites, and the consecutive reopening of the K-Ar clock of the micas.

CONCLUSIONS

New K-Ar and $^{40}Ar/^{39}Ar$ measurements on two Brazilian granites and emerald-related mineralization yield ages of about 1979 ± 28 Ma for the intrusion and cooling of the Carnaíba granite and 2032 ± 10 Ma for the first intrusive unit of the Campo Formoso granite. These data suggest that formation of emerald deposits contained in metasomatized pegmatite veins and K-metasomatites crosscutting the Jacobina volcanosedimentary series, is not separated in time from the muscovitization of the granites.

Moreover, muscovites and phlogopites from Carnaíba give similar K-Ar mean ages, 1979 ± 28 and 1973 ± 20 Ma respectively, indicating that muscovitization of granites and phlogopitization of serpentinites are synchronous. Considering the spatial distribution of the pegmatites within the upper part of the exocontact zone of the Carnaíba granitic cupola, we propose that the fluids related to the muscovitization process participated in the K-metasomatism of the serpentinites, giving rise to the emerald concentration.

The disturbed nature of $^{40}Ar/^{39}Ar$ release spectra testify to the existence of a hydrothermal heating overprinting the K-Ar clock of biotite and to a lesser extent that of phlogopite. This event is clearly subsequent to the cooling of the granites and emerald formation, and consequently is younger than 1973 ± 20 Ma.

Acknowledgements—The authors gratefully thank K. Govindaraju and M. Vernet for geochemical support, F. Saupé, A. Cheilletz, K.A. Foland and H. Maluski for the corrections of early drafts. Thanks to M. Wiedenbeck and A.M. Althoff for English and Portuguese improvements. The authors are indebted to Dr. J.L. Aronson and Dr. H.E. Gaudette that improved the manuscript by their critical review. Contribution C.N.R.S-C.R.P.G. No 1031

REFERENCES

Albarède, F., 1976. *Géochronologie comparée par la méthode $^{39}Ar/^{40}Ar$ de deux régions d'histoire post-hercynienne différente: La Montagne Noire et les Pyrénées Orientales*. Thèse d'Etat Université Paris, **7**, 158p.

Berger, G.W. and York, D.E., 1970. Precision of the $^{39}Ar/^{40}Ar$ dating technique. *Earth Planet. Sci. Lett.*, **9**, 39-44.

Berger, G.W. and York, D.E., 1981. Geothermometry from $^{40}Ar/^{39}Ar$ dating experiments. *Geochim. Cosmochim. Acta*, **45**, 795-811.

Bertrand, J.M. and Jardim de Sá, E.F., 1990. Where are the Eburnian-Transamazonian collisional belts? *Can. J. Earth Sci.*, **27**, 1382-1393.

Beus, A.A., 1966. *Geochemistry of beryllium*. W.H. Freeman Editor, 401p.

Bouseily, A.M. and El Sokhary, H.A., 1975. The relation between Rb, Ba and Sr in granitic rocks. *Chem. Geol.*, **16**, 3, 207-219.

Britos Neves, B.B., Cordani, U.G. and Torquato, J.R.F., 1980. Evolução geocronológica do Pré-cambriano do Estado da Bahia. In: Inda, H.A.V. and Duarte, F.B.: *Geologia e recursos minerais do Estado da Bahia*. Salvador S.M.E, **3**, 1-80.

Cordani, U.G. and Brito Neves, B.B., 1982. Geocronólogia do Pré-cambriano. In: Inda, H.A.V. and Barbosa, J.F.: *Texto explicativo para o mapa geológico do Estado da Bahia*, escala 1:1,000,000. Salvador, S.M.E, 32-49.

Cox, A. and Dalrymple, G.B., 1967. Statistical analysis of geomagnetic reversal data and the precision of potassium-argon dating. *Jour. Geophys. Research*, **72**, 10, 2603-2614.

Cuney, M., Sabaté, P., Vidal, Ph., Marinho, M.M. and Conceição H., 1990. The 2 Ga peraluminous magmatism of the Jacobina-Contendas Mirante belts (Bahia, Brazil): major and trace-element geochemistry and metallogenic potential. *Journ. Volc. Geother. Research*, **44**, 123-141.

Damon, P.E. and Kulp, J.L., 1958. Excess helium and argon in beryl and other minerals. *Am. Mineralogist*, **43**: 433-459.

Debon, F. and Lefort, P., 1982. A chemical-mineralogical classification of common plutonic rocks and associations. *Transactions of the Royal Society of Edimburgh: Earth Sciences*, **73**, 135-149.

Dodson, M.H., 1973. Closure temperature in cooling geochronological and petrological systems. *Contrib. Mineral. Petrol.*, **40**, 259-274.

Dunlap, W.J., Teyssier, C., McDougall, I. and Baldwin, S., 1991. Ages of deformation from K/Ar and $^{39}Ar/^{40}Ar$ dating of white micas. *Geology*, **19**, 1213-1216.

Féraud, G., Gastaud, J., Auzende, J.M., Olivet, J.L. and Cornen, G., 1982. $^{39}Ar/^{40}Ar$ ages for the alkaline volcanism and the basement of Gorringe Bank, North Atlantic Ocean. *Earth Planet. Sci. Lett.*, **57**, 211-226.

Féraud, G., York, D., Mével, C., Cornen, G., Hall, C.M. and Auzende, J.M., 1986. Additional $^{39}Ar/^{40}Ar$ dating of the basement and the alkaline voicanism of Gorringe bank, (Atlantic Ocean). *Earth Planet. Sci. Lett.*, **79**, 255-269.

Giuliani, G. and Couto, P., 1988. Emerald deposits of Brazil and its genetic link with infiltrational metasomatic process. Proceedings International Conference on "*Geochemical Evolution of the Continental Crust*", Poços de Caldas, Brazil, **1**, 236-247.

Giuliani, G., Silva, L.J.H.D. and Couto, P., 1990. Origin of emerald deposits of Brazil. *Mineralium Deposita*, **25**, 57-64.

Govindaraju, K. and Chouard, Ch., 1976. Automated optical emission spectrochemical bulk analysis of silicate rocks with microwave plasma excitation. *Anal. Chem.*, **48**, 1325-1331.

Harrison, T.M., Duncan, I and Mc Dougall, I., 1985. Diffusion of ^{40}Ar in biotite: temperature, pressure and compositional effects. *Geochim. Cosmochim. Acta*, **49**, 2461-2468.

Hess, J.C. and Lippolt, H.J., 1986. Kinetics of Ar isotopes during neutron irradiation: ^{39}Ar loss from minerals a source of error in $^{39}Ar/^{40}Ar$ dating. *Chem. Geol.*, **59**, 223-236.

Hess, J.C., Lippolt, H.J and Wirth, R., 1987. Interpretation of $^{39}Ar/^{40}Ar$ spectra of biotites: evidence from hydrothermal degassing experiments and TEM studies. *Chem. Geol*, **66**, 137-149.

Lafon, J.M., 1988. *Estudo geocronológico Rb-Sr do maciço granitico Campo Formoso, Bahia*. Relatorio FADESP, Unpublished report, 12 p.

Leutwein, F. and Kaplan G., 1963. Quelques recherches sur l'aptitude de certains cristaux de néoformation à capturer de l'argon radiogénique. *C.R. Acad. Sci.*, Paris, 257, 1315-1317.

Lo, C.H. and Onstott, T.C., 1989. ^{39}Ar recoil artifacts in chloritized biotite. *Geochim. Cosmochim. Acta*, **53**, 2697-2711.

Maluski, H., 1985. Méthode $^{39}Ar/^{40}Ar$. Principe et applications aux minéraux des roches terrestres. In: E. Roth and B. Poty (Editors), *Méthodes de datation par les phénomènes nucléaires naturels*, Masson, Paris, 341-372.

Maluski, H. and Monié, P., 1988. $^{39}Ar/^{40}Ar$ laser probe multidating inside single biotite of Variscan orthogneisses (Pinet, Massif Central, France). *Chem. Geol., Isotope geos.*, **73**, 245-263.

Mascarenhas, J.F., 1979. *Evolução geotectónica do Pré-cambriano do Estado da Bahia*. In: Geologia e recursos minerais do Estado da Bahia, Textos basicos. Inda, H.A.V. and Barbosa, J.F. (Editors), S.M.E. Salvador, 2, 55-165.

McDougall, I., Polach, H.A. and Stipp, J.J., 1969. Excess radiogenic argon in young subaerial basalts from the Auckland volcanic field, New Zealand. *Geochim. Cosmochim. Acta*, **33**, 1485-1520.

McReath, I. and Sabaté, P., 1987. Granitoids of the state of Bahia, Brazil: a review. *Revista Brasileira de Geociências*, **12**, 193-214.

Montigny, R, Le Mer, O., Thuizat, R. and Whitechurch, H., 1988. K-Ar and $^{39}Ar/^{40}Ar$ study of metamorphic rocks associated with the Oman ophiolite: tectonic implications. *Tectonophysics*, **151**, 345-362.

Moutinho da Costa, L.A. and Mascarenhas, J.F., 1982. The high-grade metamorphic terrains in the internal Mutuipe-Jequié, Archaean and Lower Proterozoic of Eastern-central Bahia. In: International Symposium "*The Archaean and Early Proterozoic geological evolution and metallogenesis*", Salvador, Brazil, 19-37.

Romano, A.W., Bertrand, J.M., Michard, A. and Zimmermann, J.L., 1991. Tectonique tangentielle et décrochements d'âge Proterozoïque inférieur (orogenèse transamazonienne, environ 2000 Ma) au Nord du "Quadrilatère ferrifère" (Minas Gerais, Brésil). *C.R. Acad. Sci. Paris*, **313**, 1195-1200.

Rudowski, L., 1989. *Pétrologie et géochimie des granites transamazoniens de Campo Formoso et Camaíba (Bahia, Brésil), et des phlogopitites à émeraudes associées*. Unpubl. Doct. Thesis Paris VI, 300 p.

Rudowski, L., Giuliani, G. and Sabaté, P., 1987. Les phlogopitites à émeraude au voisinage des granites de Campo Formoso et Carnaíba (Bahia, Brésil) : un exemple de minéralisation protérozoique à Be, Mo et W dans des ultrabasites métasomatisées. *C.R. Acad. Sci. Paris*, **301**, 18, 1129-1134.

Ruffet, G., Féraud, G. and Amouric, M., 1991. Comparison of $^{40}Ar/^{39}Ar$ conventional and laser dating of biotites from the North Trégor Batholith. *Geochim. Cosmochim. Acta*, **55**, 1675-1688.

Sabaté, P., Marinho, M.M., Vidal, Ph. and Caen-Vachette, M., 1990. The 2 Ga peraluminous magmatism of the Jacobina-Contendas Mirante belts (Bahia, Brazil): geologic and isotopic constraints on the sources. *Chem. Geol.*, **83**, 325-338.

Scherba G.N., 1970. Greisens. *Int. Geol. Rev.*, **12**, No. 2, 114-150 and No. 3, 239-255.

Schwarz, D., 1987. *Esmeraldas-inclusões em gemas*. Imprensa universitaria UFOP Ouro Preto, Brazil, 450 p.

Steiger, R. and Jaëger, E., 1977. Subcommission on geochronology: Convention on the use of decay constants in geo-and cosmochronology. *Earth Planet. Sci. Lett.*, **36**, 359-362.

Thiéblemont, D. and Cabanis, B., 1990. Utilisation d'un diagramme (Rb/100)-Tb-Ta pour la discrimination géochimique et l'étude pétrogénétique des roches magmatiques acides. *Bull. Soc. Géol. France*, **8**, T. VI, No. 1, 23-35.

Torquato, J.R., Oliveira, M.A.F.T. and Bartels, R.L., 1978. Idade radiometrica do granito de Campo Formoso, Bahia: uma idade minima para o grupo Jacobina. *Rev. Bras. Geociências*, **8**, 171-179.

Vidal, P., Marinho, M., Sabaté, P. and Vachette, M., 1989. The role of peraluminous granites to the Early Proterozoic evolution of the São Francisco craton. *Terra Cognita*, Abstracts, **1**, 179.

Vidal, P., Lasnier B. and Poirot J.P., 1992. Determination of the age and origin of emeralds using rubidium-strontium analysis. *Journ. Gemmology* **23**, 4, 198-200

Zimmermann, J.L., 1970. Contribution à l'étude de la déshydratation et de la libération de l'argon. *Geochim. Cosmochim. Acta*, **34**, 1327-1350.

Zimmermann, J.L., 1972. *L'eau et les gaz dans les principales familles de silicates*. Mémoires Sci. Terre Nancy, **22**, 188 p.

Zimmermann, J.L., Vernet, M., Guyetand, G. and Dautel, D., 1985. Données sur potassium et argon (de 1976 à 1984) dans quelques échantillons géochimiques de référence. *Géostandards Newsletter*, **9**, (2), 205-208.